Synthesis of Calix[4]resorcinarene Derivatives as Antimalarial Agents through Heme Polymerization Inhibition Assay

Rizky Riyami Putri[1], Harno Dwi Pranowo[1], Yehezkiel Steven Kurniawan[1], Hana Anisa Fatimi[2], and Jumina Jumina[1*]

[1]*Department of Chemistry, Faculty of Mathematics and Natural Sciences, Universitas Gadjah Mada, Sekip Utara, Yogyakarta 55281, Indonesia*

[2]*Department of Pharmaceutical Technology, Faculty of Pharmacy, Universitas Gadjah Mada, Sekip Utara, Yogyakarta 55281, Indonesia*

* ***Corresponding author:***

email: jumina@ugm.ac.id

Received: January 18, 2023
Accepted: July 4, 2023

DOI: 10.22146/ijc.81452

Abstract: *Malaria is an endemic disease in tropical countries, including Indonesia, with a high annual mortality rate. Because of that, serious attention shall be given to find new antimalarial agents that are highly active for medical treatment. In this work, we designed and synthesized three calix[4]resorcinarene derivatives and evaluated them as antimalarial agents through* in vitro *heme polymerization inhibitory assay. The calix[4]resorcinarenes were prepared from resorcinol and corresponding aldehyde derivatives in ethanol media through a cyclo-condensation reaction. The calix[4]resorcinarene products were obtained in 31.1–85.1% yield. The synthesized compounds were subjected to structure elucidation using spectroscopy techniques. The antimalarial activity of calix[4]resorcinarene with aromatic substituent (IC_{50} = 0.198 mg/mL) was higher than the aliphatic ones (IC_{50} = 0.282–0.814 mg/mL). It was found that all calix[4]resorcinarenes in this work exhibited stronger antimalarial activity than chloroquine diphosphate as the positive control (IC_{50} = 1.157 mg/mL). The calix[4]resorcinarenes could interact with hydrogen bonding, thus inhibiting the heme polymerization process. These findings demonstrate that calix[4]resorcinarene derivatives are potential antimalarial agents to be developed for effective medical treatment in the near future.*

Keywords: *antimalarial; aromatic; aliphatic; calix[4]resorcinarene; heme polymerization*

■ INTRODUCTION

Malaria disease is caused by *Plasmodium* infection in humans with the aid of *Anopheles* mosquitos. In 2020, it was estimated that 70% of malaria cases were generated by *P. falciparum* while 25% of active cases were caused by *P. vivax* infection. World Health Organization (WHO) reported that global malaria cases in 2020 reached 241 million in 85 countries. Among 241 million cases, 627 thousand patients died in 2020, which was higher than in 2019. The annual death number has kept increasing over the past several years. Indonesia contributed to 95 thousand active malaria cases, which is the highest number in the Southeast Asia region [1]. Therefore, serious attention shall be given to suppress death and active malaria cases in the future.

Chloroquine diphosphate, as one of the commercial antimalarial drugs, inhibits the conversion of toxic heme to hemozoin in the vacuole of *Plasmodium* parasites [2]. However, chloroquine resistance has been reported since 1950 in Africa and resistance cases are widely found recently in many countries, including Indonesia [3-4]. This resistance leads to higher chloroquine doses required in the treatment of malaria patients [5]. Unfortunately, increasing the chloroquine dose leads to serious side effects in high doses, such as headache, insomnia, nausea, diarrhea, anemia, skin itching, muscle weakness, blurred vision, difficulty

breathing, and irregular heartbeats [6-8]. Therefore, researchers are giving their best efforts to design and discover new antimalarial agents to replace chloroquine diphosphate as the standard drug [9-10]. This issue shall be handled seriously to suppress the growth of active malaria cases in the future.

Hundreds of antimalarial agents have been designed and evaluated recently [11-16]. Natural antimalarial compounds from terrestrial and marine sources have been also reported. Herlina et al. [13] reported the isolation of natural compounds from the stem bark of *Erythrina variegate*. It was found that ethyl acetate fraction exhibited antimalarial activity with a half-maximal inhibitory concentration (IC_{50}) value of 23.8 mg/mL. Further chromatographic purification process led to a well-known isoflavonoid compound named warangalone with an IC_{50} value of 4.80 mg/mL. On the other hand, the isolation of antimalarial agents from the marine sponge *Xestospongia* sp. has been reported by Murtihapsari et al. [14]. The *n*-hexane extract of *Xestospongia* sp. gave the IC_{50} value of 7.13 mg/mL. This fraction consisted of flavonoids and triterpenoids; however, detailed structure elucidation and their antimalarial activity were not reported due to the complicated separation and purification processes.

In contrast to natural compounds, the synthetic antimalarial agent is sometimes preferable due to the high purity of a single compound; thus, the researchers could understand the relationship between the chemical structure and antimalarial activity. The antimalarial of synthetic compounds, i.e., chalcones and pyrazolines, has been also reported. Chalcone derived from 4-chlorobenzaldehyde and 4-chloroacetophenone gave antimalarial activity with an IC_{50} of 98.66 mg/mL. Further functionalization of chalcone to its *N*-phenyl pyrazoline form increased its antimalarial activity (IC_{50} = 20.83 mg/mL); however, the IC_{50} value was still higher than chloroquine diphosphate (IC_{50} = 3.54 mg/mL) [15]. Other pyrazoline compounds with formyl and aryl substituents gave the IC_{50} value of 5.68–427.33 mg/mL [16].

Among the developed synthetic antimalarial drugs, calixarene derivatives attract the attention of researchers due to their ease of synthesis, high stability, and strong bioactivities [17-19]. Shah et al. [18] reported that calix[4]arene derivatives with quinoline and pyrimidine substituents gave up to 4 times lower IC_{50} value than chloroquine. In our previous study, we investigated the antimalarial activity of calixarene derivatives, named calix[4]pyrogallolarenes, through heme polymerization inhibitory assay [19]. Heme polymerization inhibitory assay was selected because the β-hematin is identic to hemozoin and β-hematin could be easily inspected in the laboratory using spectrophotometry measurement; thus, it is widely applied as an initial screening for antimalarial agents [20]. It was found that the calix[4]pyrogallolarenes gave IC_{50} values in the range of 0.238–1.268 mg/mL, which were more active than chloroquine diphosphate, which was remarkable [19]. On the other hand, calix[4]resorcinarenes belong to the metacyclophane family together with calix[4]arenes and calix[4]pyrogallolarenes with the different numbers of hydroxyl group, i.e., 4, 12 and 8 hydroxyl groups for calix[4]arenes, calix[4]pyrogallolarenes, and calix[4]resorcinarenes, respectively [17]. These variations in the numbers of hydroxyl groups may contribute to different antimalarial activities through the heme polymerization mechanism. In continuation of our research, we evaluated the antimalarial activity of the other calixarene derivatives, named calix[4]resorcinarenes, through *in vitro* heme polymerization inhibitory assay in this study.

■ EXPERIMENTAL SECTION

Materials

The used materials in this work, i.e., resorcinol ($C_6H_6O_2$), octanaldehyde ($C_8H_{16}O$), etanaldehyde (C_2H_4O), 4-nitrobenzaldehyde ($C_7H_5NO_3$), concentrated hydrochloric acid (HCl), ethanol (C_2H_5OH), glacial acetic acid (CH_3CO_2H), dimethyl sulfoxide (C_2H_6SO), sodium hydroxide (NaOH), and acetone (C_3H_6O), were purchased from Merck in pro analytical grade. Meanwhile, hematin ($C_{34}H_{33}FeN_4O_5$) and chloroquine diphosphate ($C_{18}H_{26}ClN_3{\cdot}2H_3PO_4$) were obtained from Sigma-Aldrich in pro analytical grade.

Instrumentation

The instrumentations used for the synthesis of calix[4]resorcinarenes were hotplate (ThermoScientific) and analytical balance (Shimadzu Libror EB-330). The used instrumentations for the characterization of the synthesized products were melting point apparatus (Electrothermal 9100), Fourier transforms infrared (FTIR, Thermo Scientific Nicolet iS10), liquid chromatography-mass spectrometry (LC-MS, Thermo Fischer Scientific), and nuclear magnetic resonance (500 MHz for ^{1}H- and 125 MHz for ^{13}C-NMR, JEOL JNM-ECZ 500R). On the other hand, the used apparatus for the antimalarial assay were micropipette (ThermoScientific), microcentrifuge (Thermo Sorvall Legend Micro 17R), CO_2 incubator (Sakura), vortex mixer (Thermolyne 34600 mixer), 96-well microplate (Biochemix), and ELISA reader (Bio-Rad 660 XR).

Procedure

Synthesis of calix[4]resorcinarene derivatives

The calix[4]resorcinarene was prepared in a similar manner to the previous report [21-22]. Resorcinol (5 mmol) was dissolved in ethanol (10 mL) and then acidified with concentrated HCl (0.5 mL). Aldehyde derivative (5 mmol) was added dropwise into the mixture. The mixture was stirred and refluxed for 24 h. After the reaction was completed, the mixture was cooled to room temperature and then added to distilled water (10 mL). The resulting solids were filtered and washed with a mixture of ethanol and distilled water (1:1 v/v). The melting point of the product was measured, and the product was characterized using FTIR, NMR and LC-MS analyses.

***C*-4-nitrophenylcalix[4]resorcinarene (compound 1).** Compound **1** (1.03 g) was obtained as a yellowish solid in 85.1% yield. m.p. 300 °C (decomposed). FTIR (KBr, cm^{-1}): 3448, 2924, 2854, 1604, 1512, 1350, 1427. ^{1}H-NMR (DMSO-d_6, δ, ppm): 5.73 (*s*, 4H), 6.81 (*d*, 4H), 6.86 (*s*, 4H), 7.78 (*s*, 4H), 7.84 (*d*, 4H), 8.93 (*s*, 8H). ^{13}C-NMR (DMSO-d_6, δ, ppm): 55.9, 109.0, 120.0, 122.0, 129.0, 143.0, 151.0, 162.0, 174.0. LC: major peak at a retention time of 15.12 min. Mass spectrum (EI): m/z = 971.6035 (M$^+$).

***C*-heptylcalix[4]resorcinarene (compound 2).** Compound **2** (0.83 g) was obtained as a yellowish solid in 75.5% yield. m.p. 295 °C (decomposed). FTIR (KBr, cm^{-1}): 3263, 2924, 2854, 1620, 1458. ^{1}H-NMR (DMSO-d_6, δ, ppm): 0.90 (*t*, 12H), 1.30 (*m*, 40H), 2.30 (*q*, 8H), 4.13 (*t*, 4H), 4.30 (*s*, 8H), 6.12 (*s*, 4H), 7.21 (*s*, 4H). ^{13}C-NMR (DMSO-d_6, δ, ppm): 14.1, 22.7, 25.1, 28.1, 29.6, 31.6, 33.3, 34.0, 122.0, 124.0, 150.3, 150.6. LC: major peak at a retention time of 15.17 min. Mass spectrum (EI): m/z = 879.5749 (M$^+$).

***C*-methylcalix[4]resorcinarene (compound 3).** Compound **3** (0.22 g) was obtained as a yellowish solid in 31.1% yield. m.p. 270 °C (decomposed). FTIR (KBr, cm^{-1}): 3379, 2970, 2877, 1620, 1427. ^{1}H-NMR (DMSO-d_6, δ, ppm): 1.30 (*d*, 12H), 4.46 (*q*, 4H), 6.14 (*s*, 4H), 6.78 (*s*, 4H), 8.52 (*s*, 8H). ^{13}C-NMR (DMSO-d_6, δ, ppm): 21.5, 39.0, 102.0, 123.0, 125.0, 151.0. LC: major peak at a retention time of 10.35 min. Mass spectrum (EI): m/z = 545.2211 (M+H$^+$).

In vitro *antimalarial assay*

The *in vitro* antimalarial assay was conducted using the heme polymerization inhibitory method according to the previously published procedure [19]. The heme polymerization method was performed by the addition of 1 mM hematin (100 µL) into 0.2 M NaOH solution (50 µL). The sample (50 µL) with a series concentration of 5.00, 2.50, 1.25, 0.63, and 0.31 mg/mL and glacial acetic acid (50 µL) were added into the mixture. The mixture was incubated at 37 °C for 24 h. After that, the mixture was centrifuged at 8000 rpm for 10 min. The residue was washed with dimethyl sulfoxide (200 µL). The residue was dissolved in 0.1 M NaOH solution (200 µL). The solution (100 µL) was added into a 96-well microplate to be measured with an ELISA reader at a wavelength of 405 nm. The absorbance was further converted through probit analysis to inhibitory percentage and IC_{50} value. Chloroquine diphosphate was used as the positive control while dimethyl sulfoxide 10% was used as the negative control. Each sample was subjected to triplicate measurement.

■ RESULTS AND DISCUSSION

Synthesis of Calix[4]resorcinarene Derivatives

In this work, three calix[4]resorcinarenes have been prepared from resorcinol and aldehyde derivative

which is shown in Fig. 1. The corresponding calix[4]resorcinarenes were obtained in 31.1–85.1% yield as yellowish solid from a one-pot synthetic method with ethanol as the solvent and hydrochloric acid as the catalyst. The employed aldehyde for compounds **1**, **2**, and **3** was 4-nitrobenzaldehyde, octanaldehyde, and ethanaldehyde, respectively. Different from calix[4]resorcinarenes **1** and **2**, calix[4]resorcinarene **3** was obtained in the lowest yield (31.1% yield), probably due to less stability of carbonium ions in etanaldehyde compared to aromatic aldehyde (4-nitrobenzaldehyde) and longer chain aliphatic aldehyde (octanaldehyde). It was reported that calix[4]resorcinarene was produced from the cyclo-condensation between resorcinol and aldehyde derivative in acidic conditions. According to Eddaif et al. [23], the carbonyl of aldehyde was protonated, and electrophilic substitution started to the ortho and para position of the hydroxyl groups at the aromatic ring of resorcinol. The reaction continued by the formation of its dimer and trimer and then finished when the tetramer of resorcinol was cyclized to produce a calix[4]resorcinarene structure. The proposed reaction mechanism is shown in Fig. 2.

The spectroscopic data of the synthesized products are shown in Fig. S1-S15. Calix[4]resorcinarene **1** was decomposed at 300 °C due to strong intramolecular and intermolecular hydrogen bondings as reported in other calix[4]resorcinarene derivatives [17]. The FTIR spectra of compound **1** revealed the O–H and C=C aromatic functional groups from the resorcinol at 3448 and 1604 cm^{-1}, respectively (Fig. S1). The C–H methine group was observed as weak signals at 2924 and 2854 cm^{-1} for its Csp^3–H stretching and at 1427 cm^{-1} for its C–H bending. The C–NO_2 group from the 4-nitrobenzaldehyde was confirmed by the presence of strong absorption signals at 1512 and 1350 cm^{-1}.

The ^{1}H-NMR spectrum of compound **1** in DMSO-d_6 solvent is shown in Fig. S2. The O–H of resorcinol was observed at 8.93 ppm as a singlet signal, while the aromatic protons of resorcinol were found at 6.86 and 7.78 ppm as singlet signals due to the absence of neighboring hydrogen atoms. The C–H signal of methine was confirmed by the presence of a singlet signal at 5.73 ppm, while the aromatic protons of 4-nitrobenzaldehyde were observed at 6.81 and 7.84 ppm as doublet signals. On the other hand, the ^{13}C-NMR spectrum of compound **1** in DMSO-d_6 revealed a C–H methine signal (55.9 ppm) and eight aromatic carbon signals (109.0–174.0 ppm), as shown in Fig. S3. The mass spectrum of compound 1 showed the M^+ peak at m/z = 971.6035 (Fig. S5), suggesting that the calix[4]resorcinarene structure has been formed.

Calix[4]resorcinarene **2** was decomposed at 295 °C due to intramolecular and intermolecular hydrogen bondings. Compared to the decomposition temperature of calix[4]resorcinarene **1**, calix[4]resorcinarene **2** decomposed at a lower temperature due to smaller molecular mass. The FTIR spectra of compound **2** showed the presence of O–H and C=C aromatic functional groups from the resorcinol at 3263 and 1620 cm^{-1},

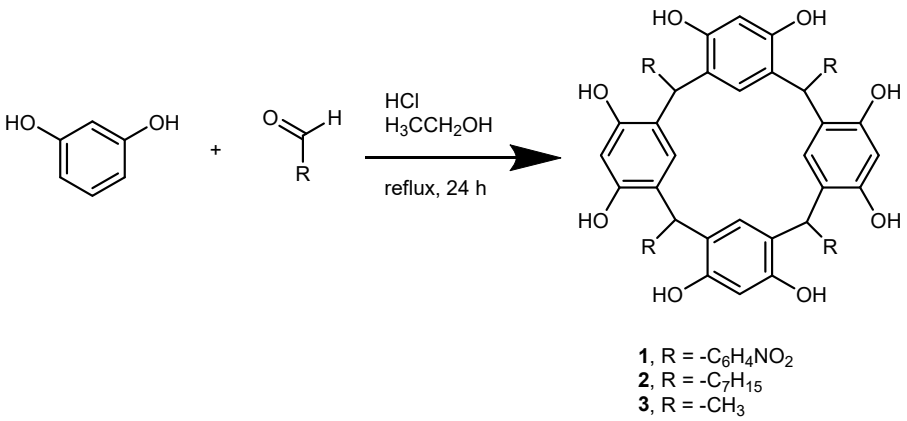

Fig 1. The synthesis scheme of calix[4]resorcinarenes

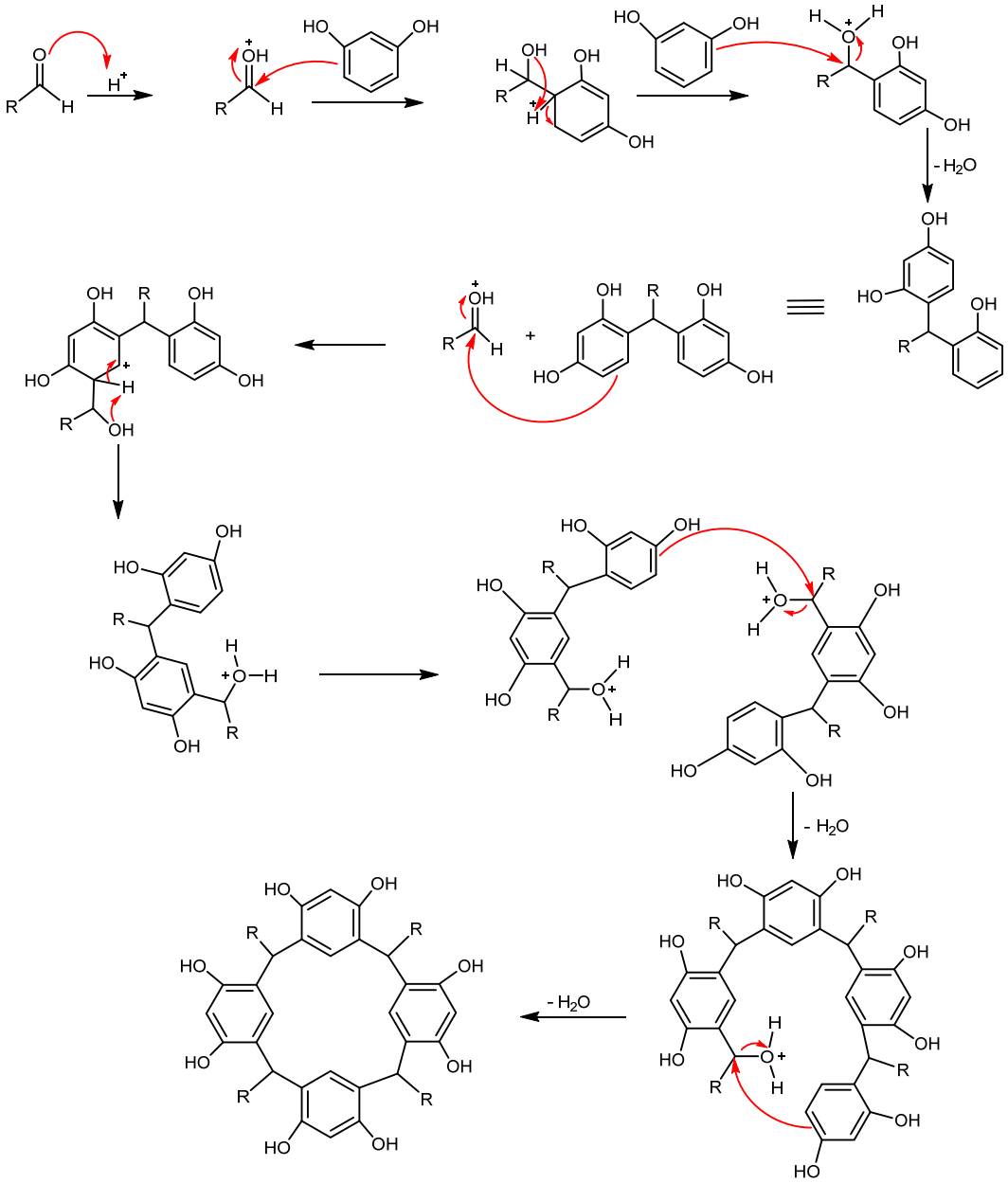

Fig 2. The proposed reaction mechanism on the synthesis of calix[4]resorcinarenes

respectively (Fig. S6). The C–H methine and *n*-heptyl groups were observed as weak signals at 2854–2924 and 1458 cm^{-1} for their bending and stretching modes, respectively.

The ^{1}H-NMR spectrum of compound **2** in deuterated DMSO solvent was displayed in Fig. S7. The O–H of resorcinol was observed at 4.30 ppm as a singlet signal, while the aromatic protons of resorcinol were found at 6.12 and 7.21 ppm as singlet signals which were similar to the spectrum of calix[4]resorcinarene **1**. The C–H signal of methine was confirmed by the presence of a triplet signal at 4.13 ppm, while the aliphatic protons of the *n*-heptyl group were found as triplet ($-CH_3$), multiplet ($-CH_2-$), and quartet ($C_{methine}-CH_2-$) signals at 0.90, 1.30 and 2.30 ppm, respectively, with a total number of 60 hydrogen atoms. On the other hand, the ^{13}C-NMR spectrum of compound **2** in DMSO-d_6 solvent confirmed the presence of a methine carbon (34.0 ppm), a methyl carbon (14.1 ppm), six methylene carbons (22.7–33.3 ppm), and four aromatic carbons (122.0–

150.6 ppm), which was matched with the total number of carbon on calix[4]resorcinarene **2** (Fig. S8). The MS spectra (Fig. S10) revealed that the M^+ signal of compound **2** was found at *m/z* = 879.5749, which was matched with its chemical formula ($C_{56}H_{80}O_8$).

On the other hand, the calix[4]resorcinarene **3** was decomposed at 270 °C, which was the lowest compared to the synthesized calix[4]resorcinarene in this work due to the smallest molecular mass as indicated by the MS spectrum (*m/z* of M^+ = 545.2211) (Fig. S15). The FTIR spectra of calix[4]resorcinarene **3** revealed the O–H and C=C aromatic functional groups from the resorcinol at 3379 and 1620 cm^{-1}, respectively (Fig. S11). The C–H of methine and methyl groups was observed as weak signals at 2970 cm^{-1} for its stretching mode and at 2877 cm^{-1} for its bending mode.

The ^{1}H-NMR spectrum of compound **3** in DMSO-d_6 as the solvent is shown in Fig. S12. The O–H of resorcinol was observed as a singlet signal at 8.52 ppm, while the aromatic protons of resorcinol were found as singlet signals at 6.14 and 6.78 ppm. The C–H proton of methine existed as a quartet signal at 4.46 ppm due to the presence of three hydrogens of methyl, which is covalently connected with the methine carbon. Meanwhile, the methyl protons were found as doublet signal at 1.30 ppm. Fig. S13 shows the ^{13}C-NMR spectrum of compound **3** in DMSO-d_6. Calix[4]resorcinarene **3** consisted of a C–H methine carbon, a methyl carbon and four aromatic carbons at 39.0, 21.5, and 102.0–151.0 ppm, respectively.

For a summary, the FTIR spectra of calix[4]resorcinarenes showed the hydroxyl functional groups at 3448–3263 cm^{-1} while C–H methine was observed at 1458–1427 cm^{-1}. The C–H methine was also observed at 4.13–5.73 and 34.0–55.9 ppm at ^{1}H- and ^{13}C-NMR, respectively. These trends were in agreement with the previous result [22]. It was reported that calix[4]resorcinarenes could be obtained in some conformations such as chair (C_4), boat (C_{2v}), chair (C_{2h}), diamond (C_s), saddle (S_4), etc., due to flexible C-C rotation on the methine bridge as reported previously [24]. The variation in the conformations of calix[4]resorcinarenes generates some peaks at the LC chromatogram (Fig. S4, S9, S14) with the same molecular ion, demonstrating that the calix[4]resorcinarenes have been successfully synthesized in the present work.

In Vitro Antimalarial Assay

Three calix[4]resorcinarenes were then evaluated as the antimalarial agent through *in vitro* heme polymerization inhibitory assay with chloroquine diphosphate as the positive control. Hematin, an artificial *Plasmodium* hemozoin, polymerizes in an acidic solution through hydrogen bonds. When this polymerization is inhibited, the heme concentration in the vacuole of the parasite will be higher, leading to the death of parasites due to the toxic properties of heme. Therefore, heme polymerization inhibitory assay is a well-established assay for rapid screening of the antimalarial activity of chemical compounds [25].

The antimalarial activity of calix[4]resorcinarenes is listed in Table 1. A series of calix[4]resorcinarene concentrations was prepared in a range of 0.31–5.00 mg/mL to obtain the average inhibition percentage for each triplicate measurement. The heme polymerization inhibition percentage was higher by increasing the used concentration of calix[4]resorcinarene. From the probit analysis, calix[4]resorcinarenes **1**, **2** and **3** gave the IC_{50} value of 0.198, 0.814, and 0.282 mg/mL, respectively.

Table 2 shows that all calix[4]resorcinarenes (IC_{50} = 0.198–0.814 mg/mL) give higher antimalarial activity than the natural extracts, i.e., *Erythrina variegate* (IC_{50} = 23.8 mg/mL), warangalone (IC_{50} = 4.80 mg/mL), and *Xestospongia* sp. (IC_{50} = 7.13 mg/mL) because natural extracts usually contain active compounds in very low concentration. Compared to the other synthetic compounds, such as chalcone (IC_{50} = 98.66 mg/mL) and pyrazolines (IC_{50} = 5.68–427.3 mg/mL), the synthesized calix[4]resorcinarenes exhibited 28.69–2158 times stronger antimalarial activity demonstrating the critical effect of calix[4]resorcinarene skeleton on the antimalarial activity.

As a family of calixarenes, the antimalarial activity of calix[4]resorcinarenes was compared with calix[4] arenes and calix[4]pyrogallolarenes. The antimalarial

Table 1. The antimalarial activity of calix[4]resorcinarenes through *in vitro* heme polymerization inhibitory assay

Calix[4]resorcinarene	Concentration	Average inhibition percentage ± SD (%)	IC_{50} (mg/mL)
1	5.00	89.28 ± 0.04	0.198
	2.50	79.56 ± 0.15	
	1.25	75.85 ± 0.25	
	0.63	69.19 ± 0.31	
	0.31	53.77 ± 0.26	
2	5.00	87.51 ± 0.18	0.814
	2.50	78.02 ± 0.39	
	1.25	65.80 ± 0.40	
	0.63	52.49 ± 0.16	
	0.31	39.47 ± 0.16	
3	5.00	85.95 ± 0.20	0.282
	2.50	80.85 ± 0.22	
	1.25	73.29 ± 0.07	
	0.63	67.35 ± 0.24	
	0.31	47.35 ± 0.15	

*SD: standard deviation

Table 2. The comparison of *in vitro* antimalarial activity of the reported antimalarial agents

Compound	IC_{50} (mg/mL)	Ref.
calix[4]resorcinarene **1**	0.198	This work
calix[4]resorcinarene **2**	0.814	
calix[4]resorcinarene **3**	0.282	
Chloroquine diphosphate	1.157	
Erythrina variegate extract	23.80	[13]
Warangalone	4.800	
Xestospongia sp. extract	7.130	[14]
chalcone	98.66	[15]
N-phenylpyrazoline	20.83	
N-formylpyrazoline	5.680	[16]
N-arylpyrazoline	427.3	
C-8-hydroxyquinolinecalix[4]arene	0.073	[18]
C-2-aminopyrimidinecalix[4]arene	0.043	
C-phenylcalix[4]pyrogallolarene	1.268	[19]
C-4-hydroxy-3-methoxyphenylcalix[4]pyrogallolarene	1.029	
C-2-chlorophenylcalix[4]pyrogallolarene	0.238	

activity of calix[4]resorcinarenes (IC_{50} = 0.198–0.814 mg/mL) was weaker than the calix[4]arenes (IC_{50} = 0.043–0.073 mg/mL). It was reported that nitrogenated functional groups such as amino, nitro, quinoline, and pyrimidine yielded stronger antimalarial activity due to stronger interactions with iron central ion in the heme framework [18]. On the other hand, the antimalarial activity of calix[4]resorcinarenes (IC_{50} = 0.198–0.814 mg/mL) was higher than calix[4]pyrogallolarenes (IC_{50} = 0.238–1.268 mg/mL) due to stronger intramolecular hydrogen bonds in calix[4]pyrogallolarenes; thus, the hydroxyl groups of calix[4]pyrogallolarenes could not strongly interact with iron cation and lowering the heme polymerization inhibitory activity [19].

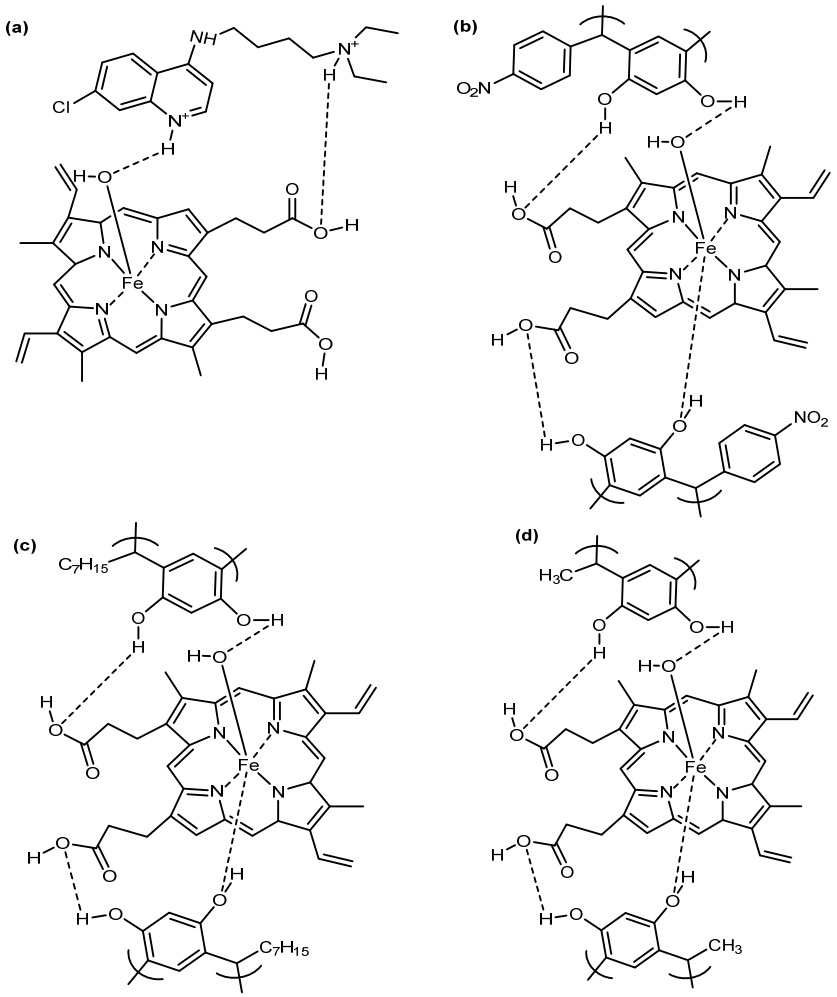

Fig 3. Plausible interactions of heme with (a) chloroquine, (b) calix[4]resorcinarene **1**, (c) calix[4]resorcinarene **2**, and (d) calix[4]resorcinarene **3**

It shall be noted that the calix[4]resorcinarenes (IC_{50} = 0.198–0.814 mg/mL) exhibited stronger antimalarial activity than chloroquine diphosphate as the positive control (IC_{50} = 1.157 mg/mL), which was remarkable. Furthermore, aromatic aldehyde moiety in compound **1** (IC_{50} = 0.198 mg/mL) exhibited stronger antimalarial activity than the aliphatic aldehyde ones (IC_{50} = 0.282–0.814 mg/mL). Meanwhile, the longer alkyl chain in compound **2** demarcated the antimalarial activity due to the non-polar nature of compound **2**. It meant that the polarity of the antimalarial agent strongly influenced its antimalarial activity. Therefore, it is reasonable that calix[4]resorcinarene **1** with nitro functional groups gave the strongest antimalarial activity in this study.

Priyangga et al. [26] reported that calix[4] resorcinarenes could form a stable chelate complex with iron metal ions through their hydroxyl groups. On the other hand, Sari et al. [19] reported that hydroxyl groups of calix[4]pyrogallolarenes interacted with iron center ion and carboxylic group of heme, thus inhibiting its polymerization process. Since calix[4]resorcinarenes' structure is similar to calix[4]pyrogallolarenes; thus, we predict that the interactions of calix[4]resorcinarenes with heme are similar to the calix[4]pyrogallolarene ones. The plausible interactions of calix[4]pyrogallolarenes and chloroquine with heme are shown in Fig. 3.

CONCLUSION

We reported the successful synthesis of three calix[4]resorcinarene derivatives in 31.1–85.1% yield. The chemical structures of all synthesized calix[4]resorcinarenes have been elucidated using FTIR, NMR, and LC-MS analyses. Besides, the *in vitro* antimalarial activity of calix[4]resorcinarenes revealed higher antimalarial activity than chloroquine diphosphate as the positive control. The type of substituent on methine carbon influenced the antimalarial activity of calix[4]resorcinarenes. Aromatic substituents gave stronger antimalarial activity than the aliphatic ones due to higher polarity. It was predicted that the calix[4]resorcinarenes interacted with heme through hydrogen bondings, thus inhibiting the heme polymerization process.

ACKNOWLEDGMENTS

The authors deeply thank to the Department of Chemistry, Faculty of Mathematics and Natural Science, Universitas Gadjah Mada, for providing financial assistance for this research through the Department Research Grant budget year 2022 with a contract number of 50/UN1/FMIPA.1.3/KP/PT.01.03/2023.

AUTHOR CONTRIBUTIONS

Conceptualization and Methodology: Jumina. Supervision: Jumina and Harno Dwi Pranowo. Resources: Jumina. Investigation: Rizky Riyami Putri. Formal analysis: Rizky Riyami Putri, Yehezkiel Steven Kurniawan and Hana Anisa Fatimi. Writing and revising the manuscript: Yehezkiel Steven Kurniawan and Hana Anisa Fatimi.

REFERENCES

[1] Oluwafemi, T., and Azuaba, E., 2022, Impact of hygiene on malaria transmission dynamics: A mathematical model, *J. Multidiscip. Appl. Nat. Sci.*, 2 (1), 1–9.

[2] Pandey, A.V., Bisht, H., Babbarwal, V.K., Srivastava, J., Pandey, K.C., and Chauhan, V.S., 2001, Mechanism of malarial haem detoxification inhibition by chloroquine, *Biochem. J.*, 355 (2), 333–338.

[3] Talapko, J., Škrlec, I., Alebić, T., Jukić, M., and Včev, A., 2019, Malaria: The past and the present, *Microorganisms*, 7 (6), 179.

[4] Pannu, A.K., 2019, Malaria today: Advances in management and control, *Trop. Doct.*, 49 (3), 160–164.

[5] Kim, J., Tan, Y.Z., Wicht, K.J., Erramilli, S.K., Dhingra, S.K., Okombo, J., Vendome, J., Hagenah, L.M., Giacometti, S.I., Warren, A.L., Nosol, K., Roepe, P.D., Potter, C.S., Carragher, B., Kossiakoff, A.A., Quick, M., Fidock, D.A., and Mancia, F., 2019, Structure and drug resistance of the *Plasmodium falciparum* transporter PfCRT, *Nature*, 576 (7786), 315–320.

[6] Veiga, M.I., Dhingra, S.K., Henrich, P.P., Straimer, J., Gnädig, N., Uhlemann, A.C., Martin, R.E., Lehane, A.M., and Fidock, D.A., 2016, Globally prevalent PfMDR1 mutations modulate *Plasmodium falciparum* susceptibility to artemisinin-based combination therapies, *Nat. Commun.*, 7 (1), 11553.

[7] Braga, C.B., Martins, A.C., Cayotopa, A.D.E., Klein, W.W., Schlosser, A.R., da Silva, A.F., de Souza, M.N., Andrade, B.W.B., Filgueira-Júnior, J.A., Pinto, W.J., and da Silva-Nunes, M., 2015, Side effects of chloroquine and primaquine and symptom reduction in malaria endemic area (Mancio Lima, Acre, Brazil), *Interdiscip. Perspect. Infect. Dis.*, 2015, 346853.

[8] Al-Bari, M.A.A., 2015, Chloroquine analogues in drug discovery: New directions of uses, mechanism of actions and toxic manifestation from malaria to multivarious diseases, *J. Antimicrob. Chemother.*, 70 (6), 1608–1621.

[9] Tse, E.G., Korsik, M., and Todd, M.H., 2019, The past, present and future of anti-malarial medicines, *Malar. J.*, 18 (1), 93.

[10] Belete, T.M., 2020, Recent progress in the development of new antimalarial drugs with novel targets, *Drug Des., Dev. Ther.*, 14, 3875–3889.

[11] Ungogo, M.A., Ebiloma, G.U., Ichoron, N., Igoli, J.O., de Koning, H.P., and Balogun, E.O., 2020, A review of the antimalarial, antitrypanosomal, and antileishmanial activities of natural compounds isolated from Nigerian flora, *Front. Chem*., 8, 617448.

[12] Nqoro, X., Tobeka, N., and Aderibigde, B.A., 2017, Quinoline-based hybrid compounds with antimalarial activity, *Molecules*, 22 (12), 2268.

[13] Herlina, T., Supratman, U., Soedjanaatmadja, M.S., Subarnas, A., Sutardjo, S., Abdullah, N.R., and Hayashi, H., 2009, Anti-malarial compound from the stem bark of *Erythrina variegate*, *Indones. J. Chem*., 9 (2), 308–311.

[14] Murtihapsari, M., Parubak, A.S., Mangallo, B., Ekasari, W., Asih, P.B., and Lestari, A.I., 2013, Isolation and presence of antimalarial activities of marine sponge *Xestospongia* sp., *Indones. J. Chem*., 13 (3), 199–204.

[15] Cahyono, R.N., Andari, S.A., and Wahyuningsih, T.D., 2022, Synthesis of *N*-phenylpyrazoline derivative from 4-chlorobenzaldehyde and 4-chloroacetophenone and its activity as an antimalarial agent, *Mater. Sci. Forum*, 1061, 211–216.

[16] Wiratama, M., Waskitha, S.S.W., Haryadi, W., and Wahyuningsih, T.D., 2022, Synthesis, antimalarial activity assay and molecular docking study of *N*-substituted chloro-pyrazolines, *Trop. J. Pharm. Res*., 21 (6), 1255–1261.

[17] Nasuhi Pur, F., 2016, Calixdrugs: Calixarene-based clusters of established therapeutic drug agents, *Mol. Diversity*, 20 (3), 781–787.

[18] Shah, R.B., Valand, N.N., Sutariya, P.G., and Menon, S.K., 2015, Design, synthesis and characterization of quinoline-pyrimidine linked calix[4]arene scaffolds as anti-malarial agents, *J. Inclusion Phenom. Macrocyclic Chem.*, 84 (1), 173–178.

[19] Sari, D.K., Hidayat, D.N.W., Fatmawati, D.R., Triono, S., Kurniawan, Y.S., and Jumina, J., 2022, Synthesis and antimalarial activity assay of *C*-arylcalix[4]pyrogallolarenes using heme polymerization inhibition activity (HPIA) method, *Mater. Sci. Forum*, 1061, 187–193.

[20] Coronado, L.M., Nadovich, C.T., and Spadafora, C., 2014, Malarial hemozoin: From target to tool, *Biochim. Biophys. Acta, Gen. Subj.*, 1840 (6), 2032–2041.

[21] Jumina, J., Priastomo, Y., Setiawan, H.R., Mutmainah, M., Kurniawan, Y.S., and Ohto, K., 2020, Simultaneous removal of lead(II), chromium(III), and copper(II) heavy metal ions through an adsorption process using *C*-phenylcalix[4]pyrogallolarene material, *J. Environ. Chem. Eng.*, 8 (4), 103971.

[22] Priyangga, K.T.A., Kurniawan, Y.S., and Yuliati, L., 2021, The role of a nitro substituent in *C*-phenylcalix[4]resorcinarenes to enhance the adsorption of gold(III) ions, *ChemistrySelect*, 6 (21), 5366–5373.

[23] Eddaif, L., Trif, L., Telegdi, J., Egyed, O., and Shaban, A., 2019, Calix[4]resorcinarene macrocycles, *J. Therm. Anal. Calorim.*, 137 (2), 529–541.

[24] Firdaus, F., Jumina, J., and Sastrohamidjojo, H., 2007, Synthesis and conformation of *p*-(amino)butoxycalix[4]arene, *Indones. J. Chem.*, 7 (1), 49–57.

[25] Basilico, N., Pagani, E., Monti, D., Olliaro, P., and Taramelii, D., 1998, A microtitre-based method for measuring haem polymerization inhibitory activity (HPIA) of antimalarial drugs, *J. Antimicrob. Chemother.*, 42 (1), 55–60.

[26] Priyangga, K.T.A., Kurniawan, Y.S., Ohto, K., and Jumina, J., 2022, A review on calixarene fluorescent chemosensor agents for various analytes, *J. Multidiscip. Appl. Nat. Sci.*, 2 (1), 23–40.

Supplementary Data

This supplementary data is a part of a paper entitled "Synthesis of Calix[4]resorcinarene Derivatives as Antimalarial Agents through Heme Polymerization Inhibition Assay".

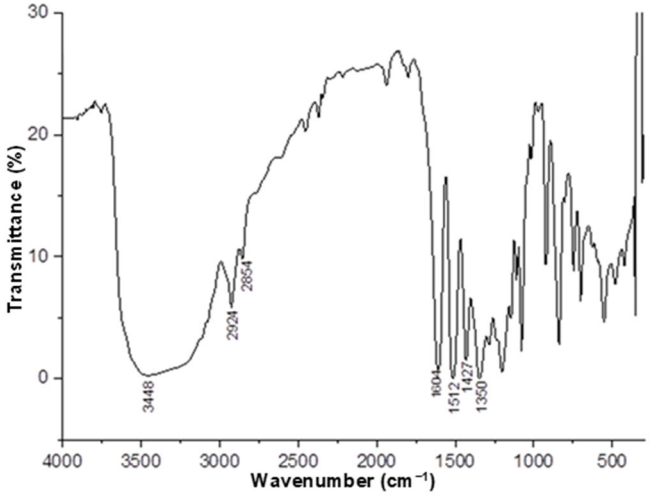

Fig S1. The FTIR spectra of calix[4]resorcinarene **1**

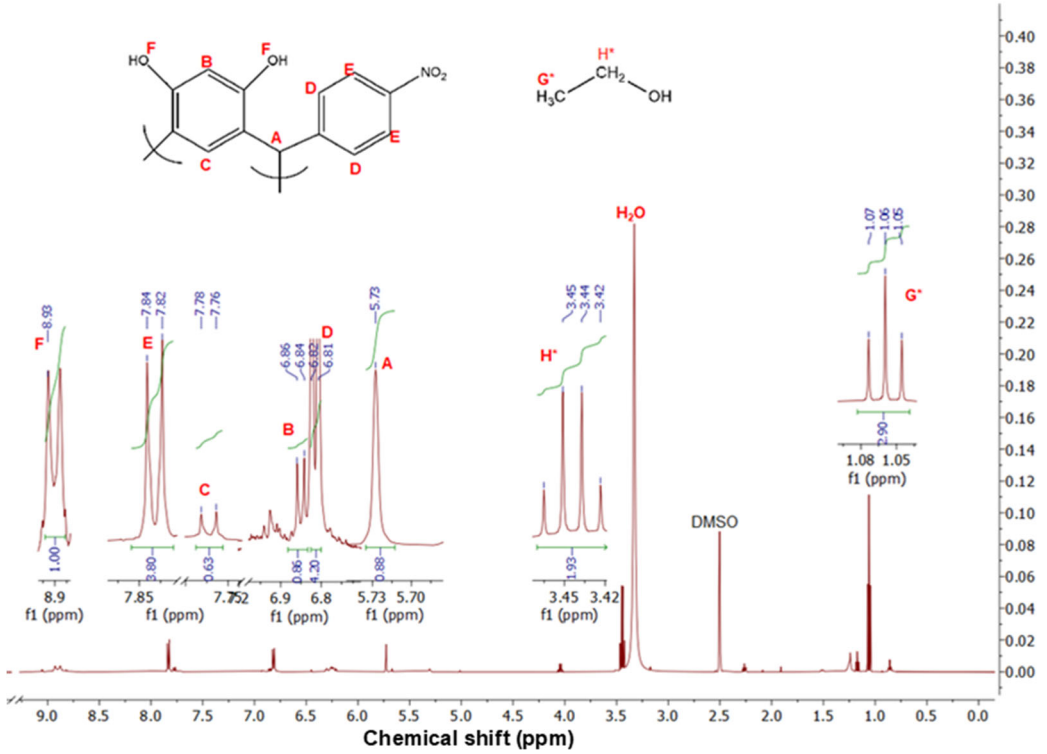

Fig S2. The ^{1}H-NMR spectra of calix[4]resorcinarene **1**

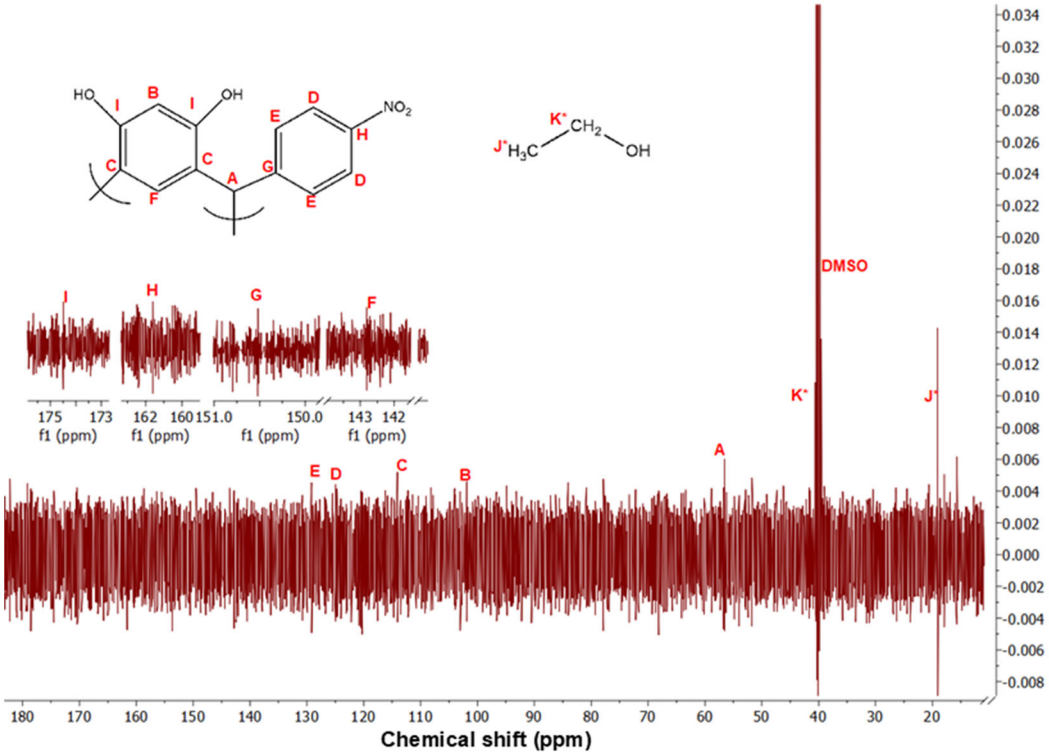

Fig S3. The ^{13}C-NMR spectra of calix[4]resorcinarene **1**

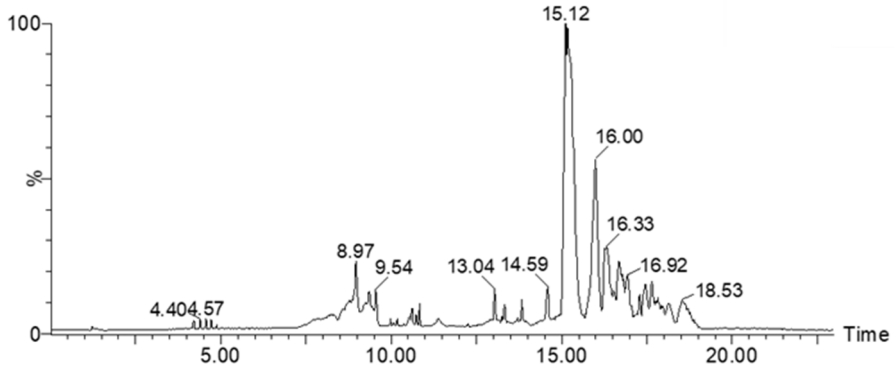

Fig S4. The LC chromatogram of calix[4]resorcinarene 1

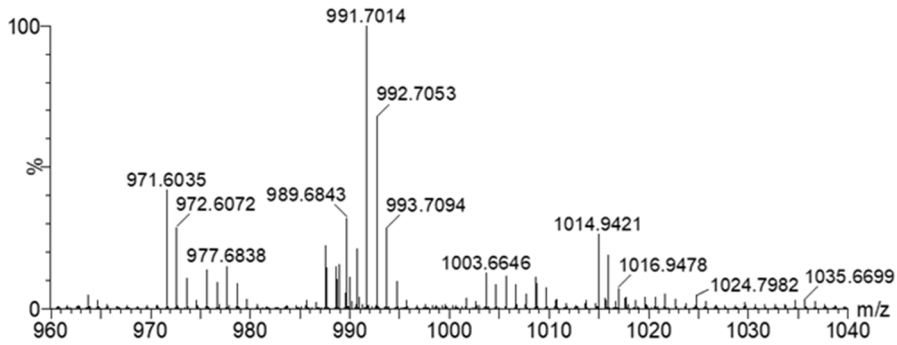

Fig S5. The MS spectra of calix[4]resorcinarene **1**

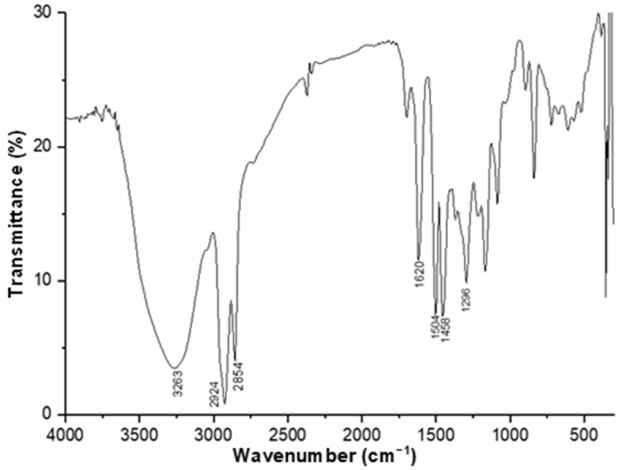

Fig S6. The FTIR spectra of calix[4]resorcinarene **2**

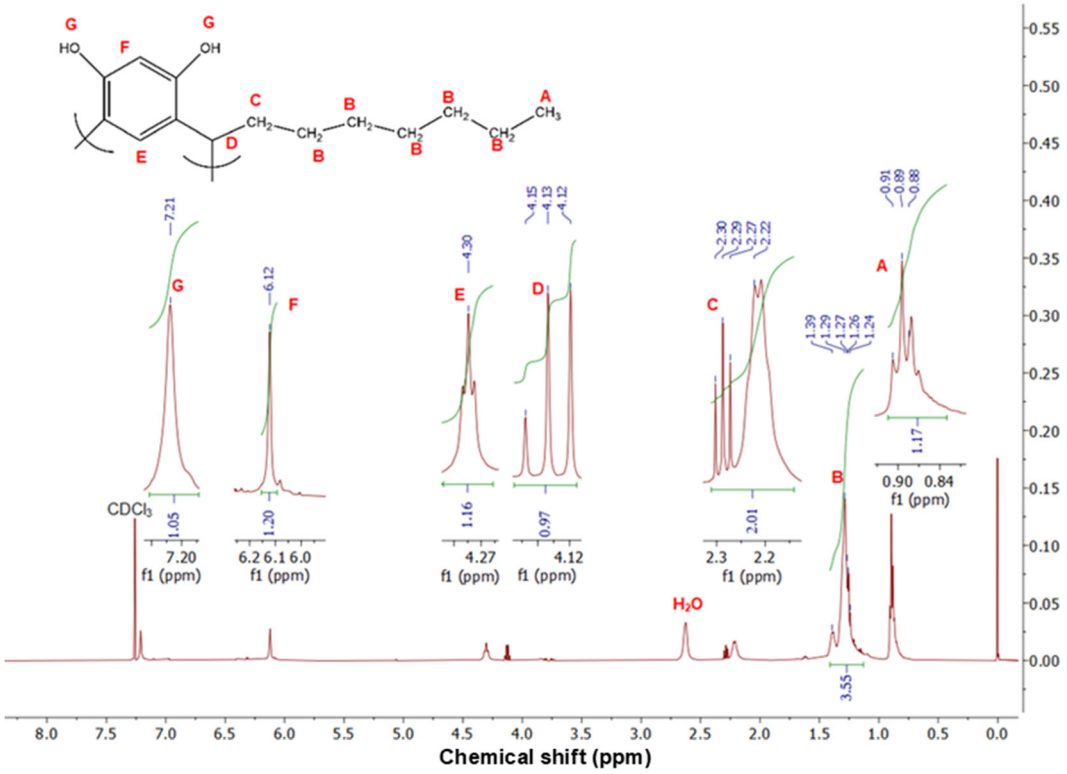

Fig S7. The ^{1}H-NMR spectra of calix[4]resorcinarene **2**

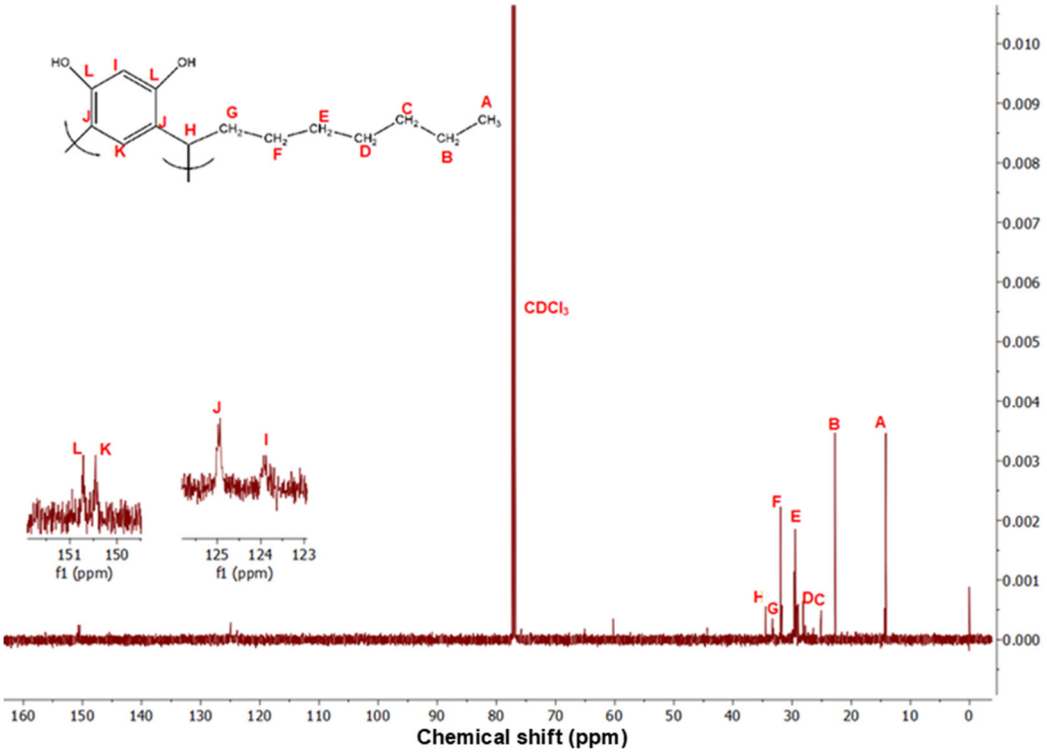

Fig S8. The ^{13}C-NMR spectra of calix[4]resorcinarene **2**

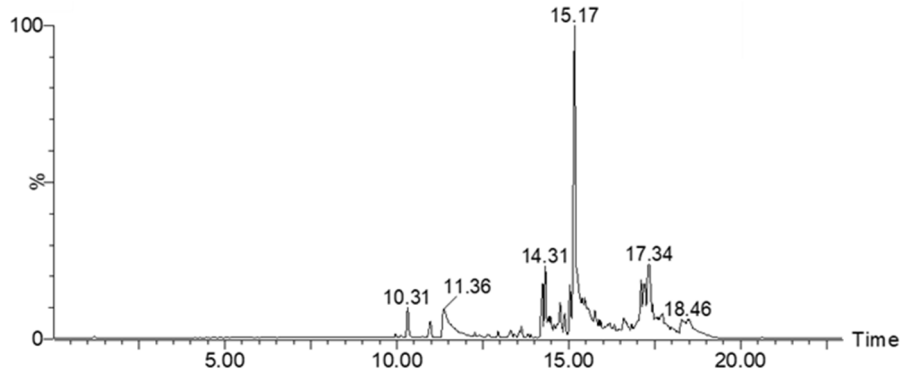

Fig S9. The LC chromatogram of calix[4]resorcinarene **2**

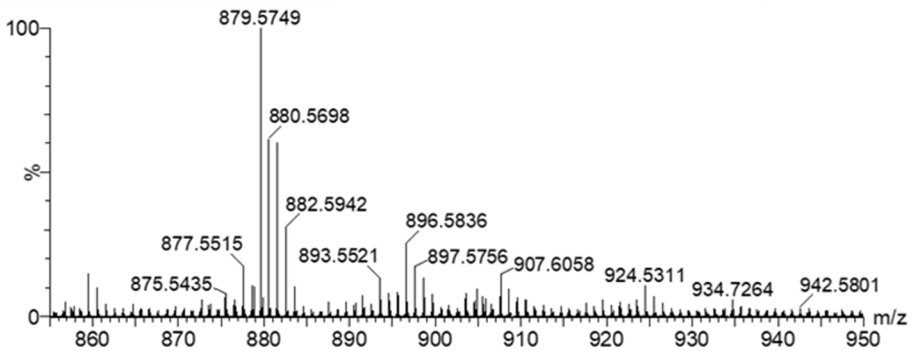

Fig S10. The MS spectra of calix[4]resorcinarene **2**

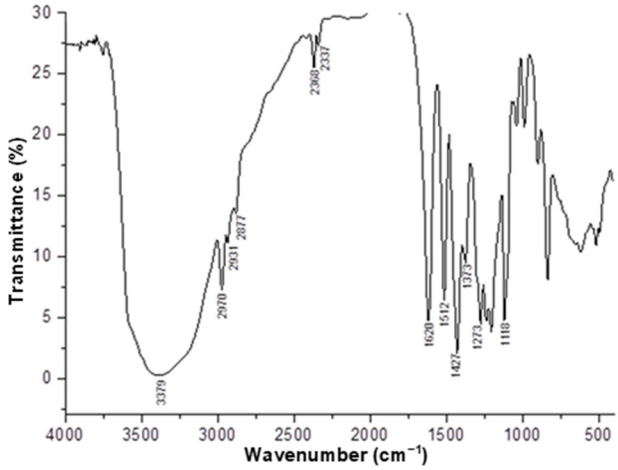

Fig S11. The FTIR spectra of calix[4]resorcinarene **3**

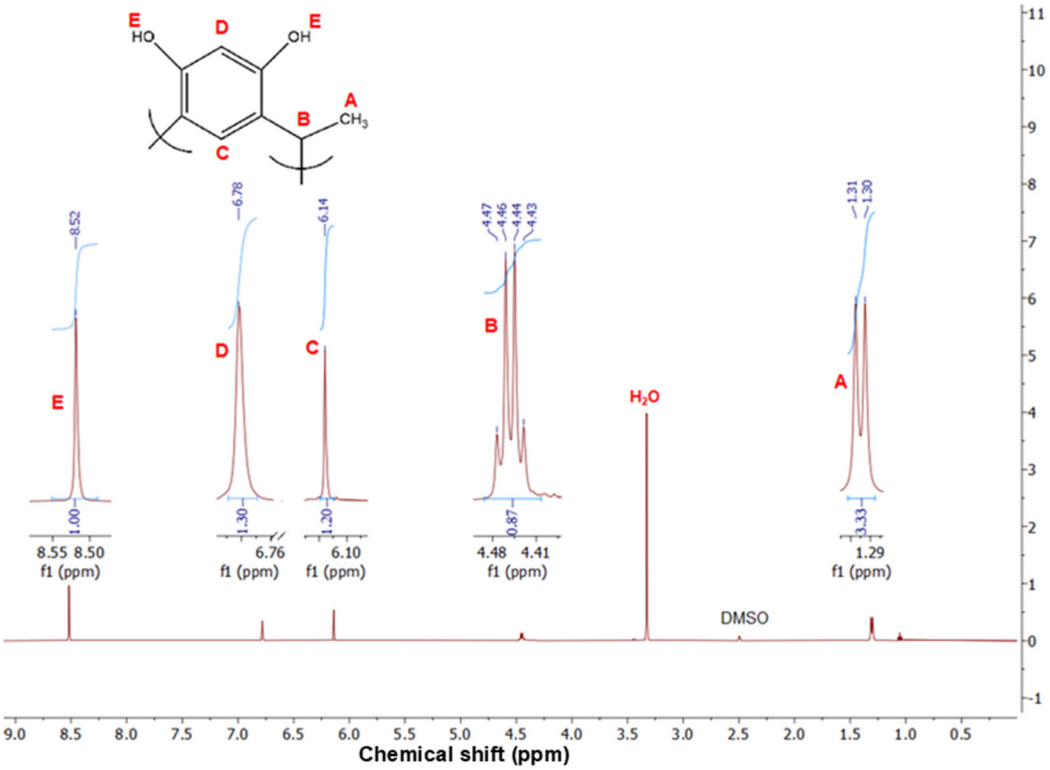

Fig S12. The ^{1}H-NMR spectra of calix[4]resorcinarene **3**

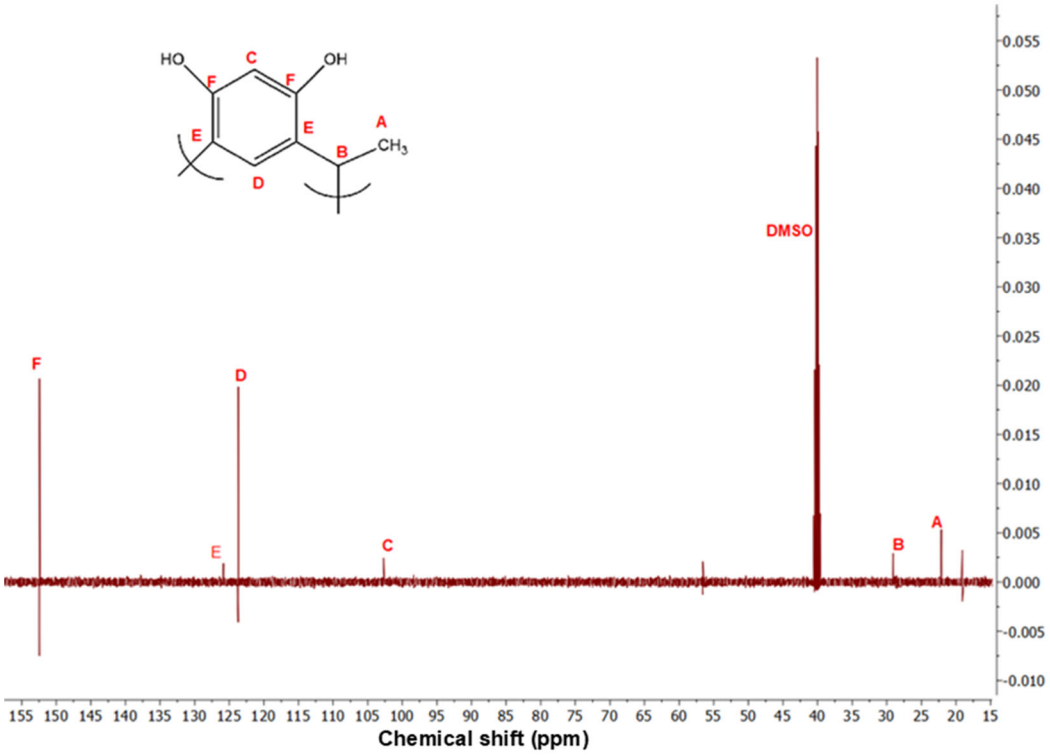

Fig S13. The ^{13}C-NMR spectra of calix[4]resorcinarene **3**

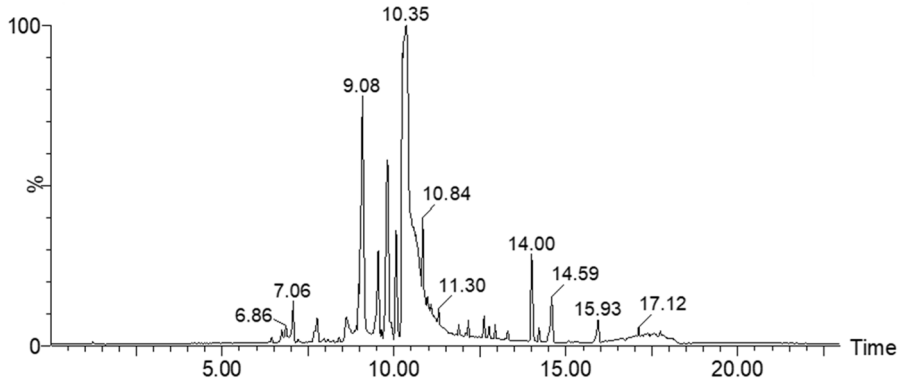

Fig S14. The LC chromatogram of calix[4]resorcinarene **3**

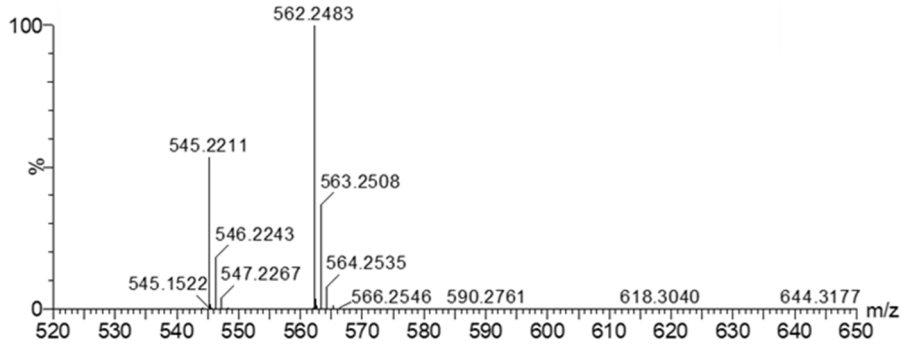

Fig S15. The MS spectra of calix[4]resorcinarene **3**